Lab on a Chip

Cite this: *Lab Chip*, 2012, **12**, 2575–2579

www.rsc.org/loc

PAPER

Continuous operation of a hybrid solid-liquid state reconfigurable photonic system without resupply of liquids†

Erica Eunjung Jung and David Erickson*

Received 22nd February 2012, Accepted 25th April 2012
DOI: 10.1039/c2lc40191f

Optofluidics offers a number of potentially transformative advantages for photonic systems. At present however there are a number of technological roadblocks that prevent the practical integration of liquid-state elements into traditional high-speed solid-state photonic systems. Two of the most important of these are the need for continuous resupply of liquids and the difficulty in shuttling light between the liquid- and solid-states. In this paper we present an integrated system that solves both these problems. For the first time we demonstrate direct evanescent and end-fire coupling between liquid- and solid-state waveguides and an on-chip fluid core/cladding separation and recirculation system that reduces the consumption of liquids more than 200 fold over the state of the art. The device is operated continuously for over 20 h without performance degradation or requiring the replenishment of liquids. We believe that our system represents an important step towards the development of practical optofluidically enabled photonic systems.

Introduction

The use of microfluidic components for light handling in optical systems was one of the early concepts that led to the formation of optofluidics[1–5] as a field. This idea has resulted in a number of novel technologies including: liquid-state optical lenses,[6–9] dye lasers,[10,11] and liquid-core/liquid-cladding optical waveguides.[12–15] Broadly speaking, the major advantages offered by liquid-state photonic elements are that: they can be physically adapted on-the-fly over very large distances, they have widely tunable optical properties, and the inherent convective processes improve heat transfer and provide better thermal stabilization.[16] Despite these advantages, it is impractical to imagine complete replacement of traditional solid-state photonic elements with liquid-state ones due their relatively low switching speed[17] and inability to perform advanced functionalities such as signal modulation[18,19] or active filtering.[20]

One approach by which one could harness the advantages of liquid-state photonic waveguides without sacrificing the performance offered by solid-state optical devices is to combine them into so-called hybrid optofluidic systems. Examples of this type of approach include the use of microfluidically adaptable liquid-state claddings for photonic crystals[21,22] and ring resonators,[23] and the use of liquid-core waveguides as physically adaptive elements in fiber-in fiber-out optical switches.[24,25] While these preliminary demonstrations, and other similar ones,[26–32] are certainly impressive, there still two major technical limitations that prevent the widespread adoption of hybrid system technology. The first is the need to continuously replenish and remove liquids from the system. Demonstrated liquid-core wave guiding systems consume liquids at rates on the order of hundreds of milliliters per day[12] making long term autonomous operation difficult. The second major limitation is the lack of an ability to shuttle light between the liquid-state element and traditional on-chip solid-state components, like ridge waveguides. While liquid-state to liquid-state[12] and liquid-state to fiber[24,25] transfer has been demonstrated, the mismatch in the physical size between a liquid waveguide and single mode solid state elements makes the physics of this transfer much more difficult for chip based photonics. In recent work, we numerically demonstrated the conditions under which it is possible to achieve this coupling.[33]

In this paper we present an integrated solution to these limitations leading towards more technologically practical hybrid photonic systems. We experimentally demonstrate and characterize the conditions for direct coupling between liquid-core and photonic waveguides on a silicon substrate and a novel fluidic recirculation system that eliminates the need for the resupply or removal of liquids. Tunable end-fire and evanescent coupling between the liquid- and solid-core waveguides are demonstrated for the first time. The fluidic recirculation system is enabled by the use of immiscible liquids and on-chip separation columns. We demonstrate 20-hour continuous operation of the reconfigurable photonic device and recirculation system (performing over 24,000 independent optical switching operations in that time with minimal performance degradation *via* the end-fire coupling over the time) and a

Sibley School of Mechanical and Aerospace Engineering, Cornell University, Ithaca, New York, 14853, USA. E-mail: de54@cornell.edu; http://nano.mae.cornell.edu; Fax: (607) 255-1222; Tel: (607) 255-4861
† Electronic supplementary information (ESI) available. See DOI: 10.1039/c2lc40191f/

200-fold reduction of the volume of used liquid compared to previous studies.[34]

Results and discussion

Device fabrication and operation

Fig. 1a–1c shows the fabrication method used to integrate the liquid and solid waveguides onto a single substrate. Briefly, standard photolithography techniques were used to fabricate a single layer of SU-8 structure that contains: the microfluidic channels to form the liquid-core waveguide, the input and output solid-core waveguides, and the separation reservoir. The patterned SU-8 layer was covered by a single PDMS sheet to seal the microfluidic channels and provide more capacity for the separation reservoir (Fig. 1c). Further details of the fabrication procedure are provided in the Methods section. The working principle of the recirculation system and a microscopic view of the actual device are shown in Fig. 1d and 1e. The recirculation was enabled by the use of immiscible liquids, DI water (RI = 1.336) as the core solution and Fluorinert electronic oil (FC-40, RI = 1.22) as the cladding. After forming the liquid waveguide, the core and cladding liquids were collected and separated in the reservoir by taking advantage of the differences in their densities and pumped back into microfluidic channels by external micropumps. Laser light (λ = 488 nm) was coupled from the input solid waveguide (labeled input SWG) to the adaptable liquid waveguide and then directed to the output solid waveguides (labeled output SWG) by controlling flow rates of the fluids (note that all experiments and data presented in this paper were obtained using pure DI water as a core fluid and the core fluid was doped with Rhodamine B dye for visualization purposes only). All fluid flows were manipulated *via* solenoid-valves which were controlled *via* a customized LabVIEW program. Details about the experimental setup are provided in the Methods section. In this paper the coupling performance was evaluated and optimized by the cross-talk parameter[35] which we defined as the ratio of the output power of the coupled solid waveguide to that of the non-coupled solid waveguide, 10 log[$P_{coupled}/P_{non\text{-}coupled}$]. Cross-talk values were calculated integrating the pixel values over the entire surface of reflectors of the solid waveguides to minimize detection errors. Although the direct measurement of the coupling loss between the liquid and solid waveguide was not made here, analysis of the coupling efficiency between liquid and solid core waveguides is provided in our earlier work.[33]

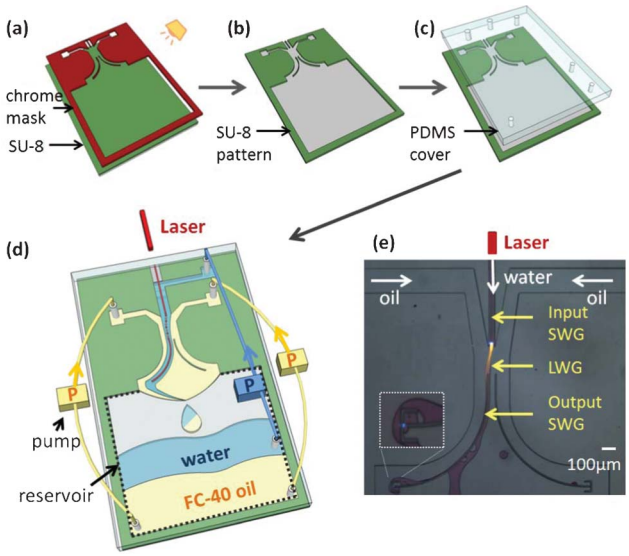

Fig. 1 Schematic showing fabrication process used to create the hybrid chip along with a view of the physical chip during end-fire coupling. (a-c) Fabrication procedure used to form solid waveguides and microchannels on the substrate. (d) Schematic showing the operation of the fluid recirculation system. (e) Microscopic view of the actual chip performing end-fire coupling between the liquid and solid waveguides with an inset showing the coupled light (λ = 488 nm). (Input and output SWG: input and output solid-core waveguides, LWG: liquid-core optical waveguide).

Liquid to solid-state end-fire coupling

Fig. 2a shows an overview of the hybrid photonic system during operation with Fig. 2b and 2c illustrating the two end-fire switching states for the liquid core waveguide. Fig. 2d shows the profile of the normalized optical intensities for the coupled (red) and non-coupled waveguides (blue) projected onto the reflectors. We observed both single mode and 2–3 modes on the reflector at the end of the coupled solid waveguide. Theoretically, the liquid waveguide with a width of 20 μm can support as many as 50 modes. Light detected at the non-coupled waveguide was caused by scattered light from the input solid waveguide and could be reduced by the adjustment of the distance between the input and the output solid waveguides. In all experiments except the experiment for Fig. 2(g), the coupled and non-coupled waveguides were located at 35 μm away from the center axis. Therefore we assumed that the radiation loss and the light coupled into the non-coupled waveguide are consistent in the experiments. Fig. 2e and 2f illustrate the range of physical

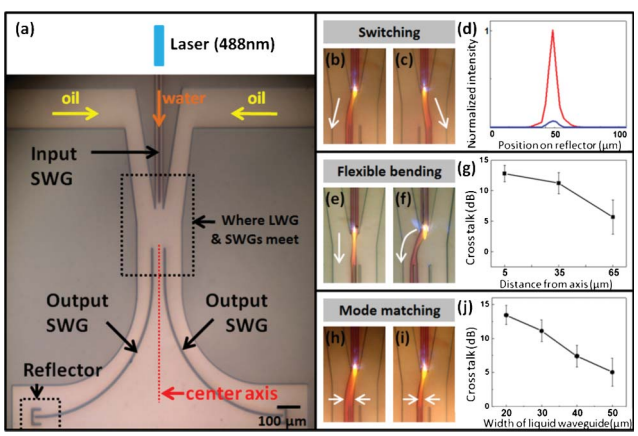

Fig. 2 Solid to liquid to solid state end-fire coupling. (a) Microscopic view of the device without the liquid waveguide. (b-c) Switching between output waveguides. Liquid waveguide was doped with Rhodamine B dye for visualization purposes. (d) Light intensity profiles of the coupled (red) and the non-coupled (blue) solid waveguide along reflectors used to obtain cross talk. (e-f) Liquid waveguides with small and large curvatures. (g) Cross-talk values as a function of the distance from the center axis to the coupled output solid waveguide. (h-i) Effect of improved mode matching between the liquid and solid waveguides. (j) Cross-talk values as a function of the width of the liquid-core waveguide.

adaptability we were able to obtain with the liquid core waveguide system. To test the effects of liquid waveguide curvature on the coupling performance, the coupled output solid waveguides were off-set between 5 μm (Fig. 2e) and 95 μm (Fig. 2f) from the center axis (equivalent to a curvature change from 10^2 to 10^3 m^{-1}) while the output solid waveguides were fixed a 35 μm from the center axis. Broadly speaking this represents a measure of the physical range over which a single element of the hybrid system can be reconfigured. Fig. 2g shows cross-talk values as a function of the offset of the output waveguide. The cross-talk value dropped from 13 dB to 6 dB when the distance is increased from 5 to 65 μm. As the curvature became larger (beyond 65 μm offset), the radiation loss from the curved liquid waveguides became severe, consistent with what one would expect with a conventional solid waveguides.[36] Fig. 2h–2i show adaptation of the width of the liquid core by changing the upstream flow conditions. This serves to change the mode profile so that it can be better matched to that of the input to the output solid core waveguide. As we decreased the applied pressure of the core flow from 70 to 17 kPa, the width of the liquid waveguide decreased from 50 to 20 μm (shown in Fig. 2j) improving the cross-talk value from 5 dB to 12 dB. Due to the modal mismatch, the scattering loss at the interface of the liquid and solid waveguides is non-negligible. This loss could be reduced in future variations of the device through geometric modifications to the solid waveguides (*e.g.* adiabatically tapered solid waveguides[37]) or modulation of the refractive index of the liquid waveguide.

Evanescent coupling

We demonstrate here evanescent coupling between liquid- and solid-core optical waveguides for the first time. Evanescent coupling is the standard method of coupling between solid-state components and is broadly used within optical telecommunication,[38,39] biosensors[40,41] and sustainable energy.[3] Demonstration of this type of coupling is therefore an important step in the development of practical hybrid systems. By controlling the pressure of the cladding flow on the left side channel in Fig. 3a, we could alter the width of the cladding flow between the liquid and the solid waveguide to change the cross-talk value. Fig. 3d and 3e show the projected light on the reflector placed at the end of the output solid waveguide and cross-talk values as a function of the pressure of the cladding flow. As expected, the coupling ratio increased as the pressure of the flow decreased to narrow the gap between the liquid and the solid waveguide. At pressures lower than 7 kPa, stable physical contact between the liquid waveguide and the solid waveguide was obtained as shown in Fig. 3b and 3c. We refer to this here as contact coupling. In contact coupling, the liquid waveguide becomes the cladding for the solid core after transferring light directly to the solid waveguide. When the evanescent coupling state transforms to the contact coupling state, the liquid waveguide contacts the solid waveguide resulting in no downstream flow of the left cladding stream as shown in Fig. 3c and fig. S1. The transition from the evanescent to contact coupling resulted in a sudden increase of the cross-talk (6 dB to 10 dB). Unlike the evanescent coupling in which the coupling ratio is determined by the propagation constants of the liquid and solid waveguides, contact coupling directly transmits light across the liquid-solid interface and therefore tends to be more efficient.

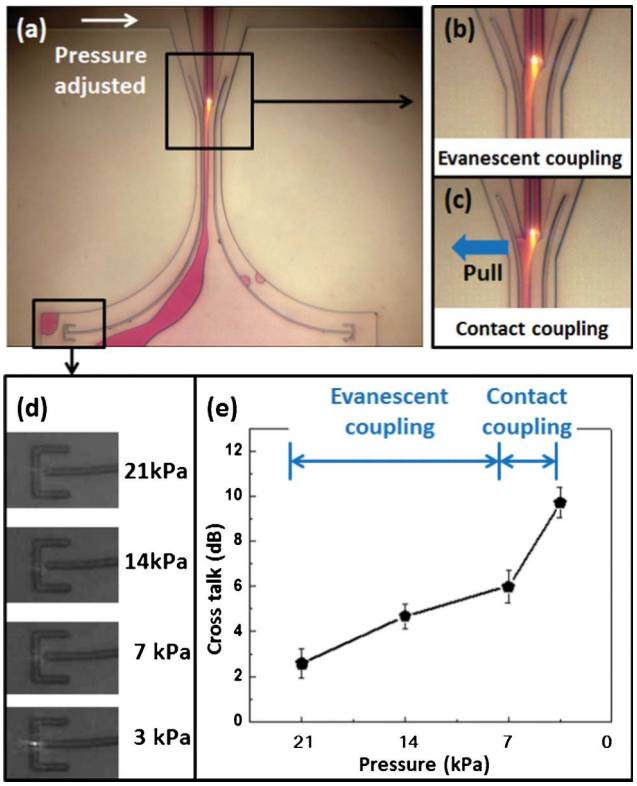

Fig. 3 Evanescent coupling between liquid-state and solid-state waveguides. (a) Image showing a chip during coupling. (b–c) Magnified view of evanescent and contact coupling. (d) Images of the coupled light projected on the reflector as a function of the pressure of the cladding flow. (e) Cross talk values as a function of the pressure of the cladding flow showing the cross over between evanescent and contact coupling.

Continuous recirculation system and demonstration of long term operation

Fluidic recirculation is fundamentally important to the development of a practical hybrid system as it allows one to operate the device continuously without having to refill or remove liquids from the chip. To demonstrate the long-term operation of our device we performed the end-fire optical switching for 20 continuous hours, without requiring the resupply of liquids. As above, we measured the system performance using cross-talk values at different switching speeds (1 s, 3 s, and 5 s). The results are shown in Fig. 4. Supporting videos S1 and S2 show the repeated optical switching *via* the end fire coupling mode as observed from inside and outside the chip respectively. The fastest reconfiguration speed we could obtain was on the order of one hundred milliseconds due to the limitation in response time of the pressure-driven flow. Fig. 4a shows images of the end fire coupling at the start and at the end of the 20 h operational period at 1 s switching speed and Fig. 4b shows the cross talk values measured periodically during the operation. The cross-talk values increased for slower switching periods due to the more precise alignment between the liquid and solid waveguides (*i.e.* at faster switching speeds the liquid waveguide did not have time to fully settle into the optimal coupling position). No significant

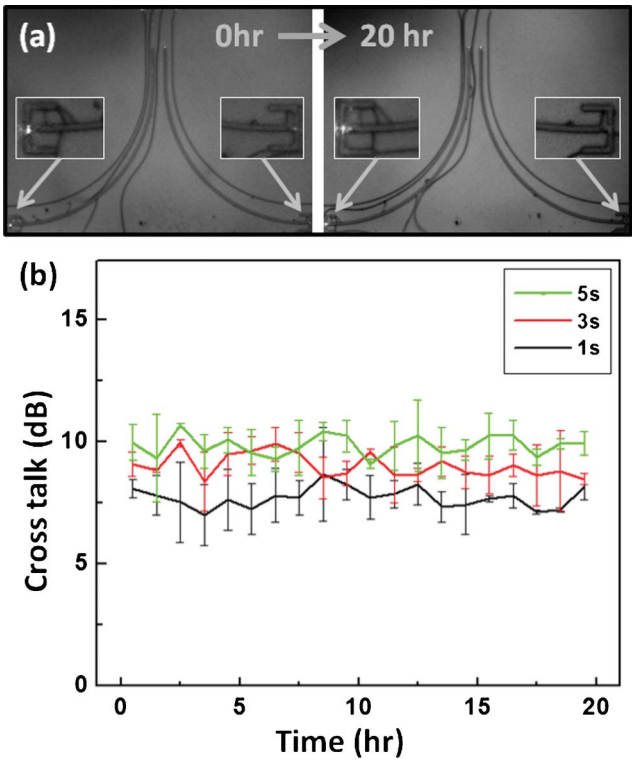

Fig. 4 Demonstration of continuous 20-hour operation of the recirculation system. (a) Images showing end fire coupling at the start and the end of the 20-hour experiment respectively. Insets: Magnified view of reflectors where coupled lights are projected on. (b) Cross talk values with different switching speeds (1, 3, and 5 s) as a function of time.

degradation was observed over the course of the operation for all switching speeds. While the recirculation system was capable of performing for longer durations, the experiment was stopped after 20 h due to the thermal damage on the input solid waveguide that couples light into the chip. Over 20 h, the system consumed about 200 μL of working fluids due to a combination of evaporation and absorption by the permeable PDMS. This loss is not fundamental to the approach but more of a consequence of the imperfect materials we used in the prototype. Better material selection could reduce this to zero consumption. The liquid consumption compares with the 40 mL/20 h of liquid consumed by the device presented in Lim *et al.*[34] for the same time period, representing 200-fold improvement. The chip itself has a capacity of approximately 1 mL of liquid (0.5 mL of oil and 0.5 mL of water) in the separation column. Even including the non-consumed portion of the fluid stored on the chip (1.2 mL), this represents about 33 fold improvement over these previous works.

Conclusions

In this work, we have taken an important step towards the development of practical hybrid optofluidic photonic systems by demonstrating: the direct coupling between liquid-core waveguides and solid-state waveguides, and an on-chip fluidic recirculation system that vastly reduces the need for liquid replenishment enabling us to operate the devices for an extended period. We note that while the microfluidic reconfiguration demonstrated here is too slow to be used for direct signal modulation, there are a number of advantages that physical reconfiguration of the waveguiding structure enables. One of the major advantages of the physical reconfiguration of the waveguiding structure demonstrated here is that it is inherently broadband enabling the routing of light more or less independent of wavelength. Solid state methods of switching mostly rely on exploiting relatively weak refractive index modulation techniques (such as thermo-optic,[42] acousto-optic,[43,44] and electro-optic effects) which must be enhanced through the use of optical resonance. Incorporating resonance necessarily narrows the range of wavelengths that can be modulated. Although physical tunability can also be obtained by micro-opto-electro-mechanical systems (MOEMS[45,46]), the advantage of using fluidic systems are the range of physical tunability that can be obtained (100 s of micrometers) and the lack of a need to define optical elements (*e.g.* evanescent couplers) *a prior*. Generally speaking though, the most severe limitation of optofluidic systems to date has been the need to continuously supply and remove liquids from the devices. A non-circulating device which consumes 48 mL of liquid over the course of a day[34] would require the replacement and disposal of over 0.3 L of liquid each week and 17 liters over the course of a year for each element. Our demonstration of a recirculation technique that largely eliminates this need and enables of long term operation of the device without significant performance degradation is an important step towards creating practical fluid-optical systems.

Methods

Fabrication

The fabrication procedure is shown in Fig. 1(a–c). Briefly, the silicon dioxide layer was grown on a silicon wafer using GSI plasma enhanced chemical vapor deposition system. SU-8 2015 (permanent epoxy negative photoresist, Microchem) was spun at 1500 rpm for 40 s on the silicon dioxide layer to achieve a film thickness of 30 μm. Exposure of the wafer was done using a contact lithography tool and the cured photoresist was developed using a 1-Methoxy-2-propyl acetate solution (*SU-8* Developer, Microchem). The device was then diced and cleaved using a partial backside cleaving technique to create a clean coupling edge for solid waveguides on the silicon substrate. Finally, the whole structure was covered by a sheet of PDMS (Sylgard® 184 Elastomer Kit, Dow Corning) to complete microchannels and the separation reservoir. Oxygen plasma treatment was used to bond the PDMS cover to the SU-8 structure.

Experimental setup

The device was mounted on the customized vertical alignment setup to separate oil (3 M Fluorinert electronic liquid FC-40, density = 1855 kg m^{-3}) and water (density = 1000 kg m^{-3}) in the separation reservoir. Laser light (λ = 488 nm) was coupled from a single mode optical fiber (Thorlabs SM450) to the input solid waveguide through the free-space coupling. Images were recorded by a CCD camera (**Sony XCD-X710 Firewire**) mounted on the vertical microscope setup. Optical power coupled into the

output solid waveguides was visualized by micro reflectors fabricated at the end of output solid waveguides.

Acknowledgements

This work was partially supported by the Air Force Office of Scientific Research through an STTR grant to Illuminaria LLC. under the Reconfigurable Materials for Cellular Electronic and Photonic Systems discovery challenge thrust, and by the US National Science Foundation through grant NSF-CBET-0846489 "CAREER: Optofluidics - Fusing Microfluidics and Photonics." The authors appreciate access and the use of the facilities of the Cornell Nanofabrication Facility (CNF).

References

1 D. Psaltis, S. R. Quake and C. H. Yang, *Nature*, 2006, **442**, 381–386.
2 C. Monat, P. Domachuk and B. J. Eggleton, *Nat. Photonics*, 2007, **1**, 106–114.
3 D. Erickson, D. Sinton and D. Psaltis, *Nat. Photonics*, 2011, **5**, 583–590.
4 H. Schmidt and A. R. Hawkins, *Nat. Photonics*, 2011, **5**, 598–604.
5 X. D. Fan and I. M. White, *Nat. Photonics*, 2011, **5**, 591–597.
6 T. Krupenkin, S. Yang and P. Mach, *Appl. Phys. Lett.*, 2003, **82**, 316–318.
7 L. Pang, U. Levy, K. Campbell, A. Groisman and Y. Fainman, *Opt. Express*, 2005, **13**, 9003–9013.
8 X. L. Mao, J. R. Waldeisen, B. K. Juluri and T. J. Huang, *Lab Chip*, 2007, **7**, 1303–1308.
9 S. K. Y. Tang, C. A. Stan and G. M. Whitesides, *Lab Chip*, 2008, **8**, 395–401.
10 Z. Y. Li, Z. Y. Zhang, T. Emery, A. Scherer and D. Psaltis, *Opt. Express*, 2006, **14**, 696–701.
11 W. Z. Song and D. Psaltis, *Appl. Phys. Lett.*, 2010, 96.
12 D. B. Wolfe, R. S. Conroy, P. Garstecki, B. T. Mayers, M. A. Fischbach, K. E. Paul, M. Prentiss and G. M. Whitesides, *Proc. Natl. Acad. Sci. U. S. A.*, 2004, **101**, 12434–12438.
13 Y. C. Seow, S. P. Lim and H. P. Lee, *Appl. Phys. Lett.*, 2009, 95.
14 K. S. Lee, S. B. Kim, K. H. Lee, H. J. Sung and S. S. Kim, *Appl. Phys. Lett.*, 2010, 97.
15 Y. Yang, A. Q. Liu, L. Lei, L. K. Chin, C. D. Ohl, Q. J. Wang and H. S. Yoon, *Lab Chip*, 2011, **11**, 3182–3187.
16 U. Levy and R. Shamai, *Microfluid. Nanofluid.*, 2008, **4**, 97–105.
17 A. Hache and M. Bourgeois, *Appl. Phys. Lett.*, 2000, **77**, 4089–4091.
18 Q. F. Xu, B. Schmidt, S. Pradhan and M. Lipson, *Nature*, 2005, **435**, 325–327.
19 J. S. Levy, A. Gondarenko, M. A. Foster, A. C. Turner-Foster, A. L. Gaeta and M. Lipson, *Nat. Photonics*, 2010, **4**, 37–40.
20 H. G. Park, C. J. Barrelet, Y. N. Wu, B. Z. Tian, F. Qian and C. M. Lieber, *Nat. Photonics*, 2008, **2**, 622–626.
21 D. Erickson, T. Rockwood, T. Emery, A. Scherer and D. Psaltis, *Opt. Lett.*, 2006, **31**, 59–61.
22 C. L. C. Smith, U. Bog, S. Tomljenovic-Hanic, M. W. Lee, D. K. C. Wu, L. O'Faolain, C. Monat, C. Grillet, T. F. Krauss, C. Karnutsch, R. C. McPhedran and B. J. Eggleton, *Opt. Express*, 2008, **16**, 15887–15896.
23 U. Levy, K. Campbell, A. Groisman, S. Mookherjea and Y. Fainman, *Appl. Phys. Lett.*, 2006, 88.
24 A. J. Chung and D. Erickson, *Opt. Express*, 2011, **19**, 8602–8609.
25 J. M. Lim, J. P. Urbanski, T. Thorsen and S. M. Yang, *Appl. Phys. Lett.*, 2011, 98.
26 S. Campopiano, R. Bernini, L. Zeni and P. M. Sarro, *Opt. Lett.*, 2004, **29**, 1894–1896.
27 S. Balslev and A. Kristensen, *Opt. Express*, 2005, **13**, 344–351.
28 L. Diehl, B. G. Lee, P. Behroozi, M. Loncar, M. A. Belkin, F. Capasso, T. Aellen, D. Hofstetter, M. Beck and J. Faist, *Opt. Express*, 2006, **14**, 11660–11667.
29 H. Y. Zhu, I. M. White, J. D. Suter, P. S. Dale and X. D. Fan, *Opt. Express*, 2007, **15**, 9139–9146.
30 D. L. Yin, E. J. Lunt, M. I. Rudenko, D. W. Deamer, A. R. Hawkins and H. Schmidt, *Lab Chip*, 2007, **7**, 1171–1175.
31 A. Y. Lau, L. P. Lee and J. W. Chan, *Lab Chip*, 2008, **8**, 1116–1120.
32 E. Schonbrun, P. E. Steinvurzel and K. B. Crozier, *Opt. Express*, 2011, **19**, 1385–1394.
33 E. E. Jung, A. J. Chung and D. Erickson, *Opt. Express*, 2010, **18**, 10973–10984.
34 J. M. Lim, S. H. Kim, J. H. Choi and S. M. Yang, *Lab Chip*, 2008, **8**, 1580–1585.
35 M. R. Phillips and D. M. Ott, *J. Lightwave Technol.*, 1999, **17**, 1782–1792.
36 C. R. Pollock, *Richard D. Irwin, INC.*, 1995.
37 K. Kasaya, O. Mitomi, M. Naganuma, Y. Kondo and Y. Noguchi, *IEEE Photonics Technol. Lett.*, 1993, **5**, 345–347.
38 F. Chollet, M. de Labachelerie and H. Fujita, *IEEE J. Sel. Top. Quantum Electron.*, 1999, **5**, 52–59.
39 H. L. R. Lira, S. Manipatruni and M. Lipson, *Opt. Express*, 2009, **17**, 22271–22280.
40 S. Blair and Y. Chen, *Appl. Opt.*, 2001, **40**, 570–582.
41 A. H. J. Yang, S. D. Moore, B. S. Schmidt, M. Klug, M. Lipson and D. Erickson, *Nature*, 2009, **457**, 71–75.
42 E. A. Camargo, H. M. H. Chong and R. M. De la Rue, *Opt. Express*, 2004, **12**, 588–592.
43 F. Verluise, V. Laude, Z. Cheng, C. Spielmann and P. Tournois, *Opt. Lett.*, 2000, **25**, 575–577.
44 N. Courjal, S. Benchabane, J. Dahdah, G. Ulliac, Y. Gruson and V. Laude, *Applied Physics Letters*, 2010, 96.
45 L. Y. Lin, E. L. Goldstein and R. W. Tkach, *J. Lightwave Technol.*, 2000, **18**, 482–489.
46 L. Y. Lin and E. L. Goldstein, *IEEE J. Sel. Top. Quantum Electron.*, 2002, **8**, 163–172.